Materials Research Bulletin 67 (2015) 83–86

Contents lists available at ScienceDirect

Materials Research Bulletin

journal homepage: www.elsevier.com/locate/matresbu

Structure and properties of $Pb(Lu_{1/2}Nb_{1/2})O_3$–$0.2PbTiO_3$ relaxor ferroelectric crystal

Ying Liu [a,c], Xiaoming Yang [b,c], Fachun Lai [a,**], Zhigao Huang [a], Xiuzhi Li [c], Zujian Wang [c], Chao He [c], Ju Lin [c], Xifa Long [c,*]

[a] College of Physics and Energy, Fujian Normal University, Fuzhou, Fujian 350117, China
[b] College of Materials Science and Engineering, Fujian Normal University, Fuzhou, Fujian 350117, China
[c] Key Laboratory of Optoelectronic Materials Chemistry and Physics, Fujian Institute of Research on the Structure of Matter, Chinese Academy of Sciences, Fuzhou, Fujian 350002, China

ARTICLE INFO

Article history:
Received 4 December 2014
Received in revised form 13 February 2015
Accepted 3 March 2015
Available online 5 March 2015

Keywords:
B. Crystal growth
D. Crystal structure
D. Electrical properties

ABSTRACT

Ferroelectric crystal $Pb(Lu_{1/2}Nb_{1/2})O_3$–$0.2PbTiO_3$ (PLN–0.2PT) was successfully obtained by a top-seed solution growth technique. At room temperature the symmetry was orthorhomic according to X-ray diffraction (XRD). The super-lattice reflections were identified by XRD and transmission electron microscope (TEM). The micro-domain structure was detected by TEM. The temperature dependence of the dielectric constant (ε') shows a typical relaxor behavior. The temperature dependence of coercive electric field and remnant polarizations were investigated, which also shows the relaxor feature.

1. Introduction

Relaxor ferroelectrics or relaxors are a class of materials which possess peculiar structure and exhibits characteristic dielectric behavior with diffuse permittivity peaks. These peaks depend strongly on frequency compared with other normal ferroelectrics [1–4]. One view of relaxors is the existence of polar nanoregions (PNRs) or polar clusters, which can give rise to many specific properties [4–6]. The PNRs or polar clusters, can be thought as unusually large dipoles, whose direction and magnitude depend on the external electric field applied [6]. The relaxor behavior was first observed in the perovskites with disorder of non-isovalent ions such as $Pb(Mg_{1/3}Nb_{2/3})O_3$ (PMN) [7] and $Pb(Sc_{1/2}Ta_{1/2})O_3$ (PST) [8].

$PbTiO_3$-based relaxor ferroelectric (PT-based relaxors) crystals with complex perovskite structure formula $(1-x)Pb(B_1,B_2)O_3$–$xPbTiO_3$ ($B_1 = Mg^{2+}$, Zn^{2+}, Sc^{3+}, In^{3+}, Yb^{3+} . . . , $B_2 = Nb^{5+}$, Ta^{5+}, W^{6+} . . .) have been the subject of intense research for the past several decades because of their interesting physical properties and potential applications in electronic devices. The typical examples are $Pb(Mg_{1/3}Nb_{2/3})O_3$–$PbTiO_3$ (PMNT) [9–11] and $Pb(Zn_{1/3}Nb_{2/3})O_3$–$PbTiO_3$ (PZNT) [12–14], which exhibits remarkably high piezoelectric properties with low Curie temperature T_C (<170 °C) and relative low depoling temperature T_{RT} (<100 °C). Although PT-based relaxors were first reported nearly half a century ago, this field of research has experienced a revival of interest in recent years respect to the enhancement of the Curie temperature and depoling temperature. Example of these work include and not limited to $Pb(Yb_{1/2}Nb_{1/2})O_3$–$PbTiO_3$ (PYNT) [15,16], $Pb(Sc_{1/2}Nb_{1/2})O_3$–$PbTiO_3$ (PSNT) [17–19], $Pb(In_{1/2}Nb_{1/2})O_3$–$PbTiO_3$ (PINT) [20,21] and $Pb(Lu_{1/2}Nb_{1/2})O_3$–$PbTiO_3$ (PLNT) [22–26].

PLN–*x*PT ceramics have been investigated in the past few years. Antonova et al. reported the PLN–*x*PT ceramics system obtained by solid phase reactions, which has a MPB region in the range of $x = 0.38$–0.49 from a pseudomonoclinic (space group Bmm2) to tetragonal (space group P4mm) at room temperature [24]. The compositions within the MPB region show high Curie temperature ($T_C = 353$ °C) and good piezoelectric properties ($k_p = 0.66$, $k_t = 0.48$) [25]. Recently, the PLN–PT ceramics were also studied by Shen et al. in our laboratory [22]. The phase structure at room temperature changes from rhombohedral (space group R3m) to tetragonal (space group P4mm). The Curie temperature of the composition $x = 0.48$ is up to 375 °C and show good piezoelectric properties ($d_{33} = 350$ pC/N) [22]. The high Curie temperature and moderate piezoelectric coefficient of the PLN–PT system imply that the PLN–PT single crystal can be a promising material for high power transducer that has a wide working temperature range. Therefore, a series of PLN–*x*PT binary ferroelectric crystals were successfully obtained firstly by top-seed solution growth technique in our lab

* Corresponding author. Tel.: +86 591 83710369; fax: +86 591 83704907.
** Corresponding author. Tel.: +86 591 22868137; fax: +86 591 22868132.
E-mail addresses: laifc@fjnu.edu.cn (F. Lai), lxf@fjirsm.ac.cn (X. Long).

http://dx.doi.org/10.1016/j.materresbull.2015.03.005
0025-5408/

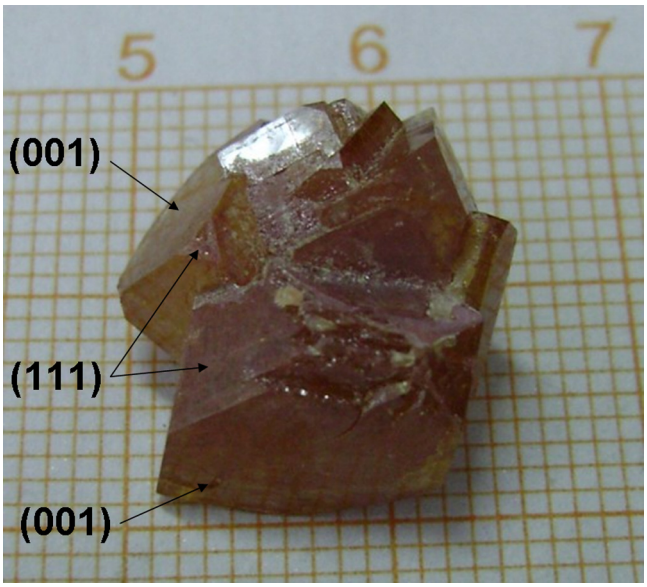

Fig. 1. As-grown PLN–0.2PT single crystal using TSSG method.

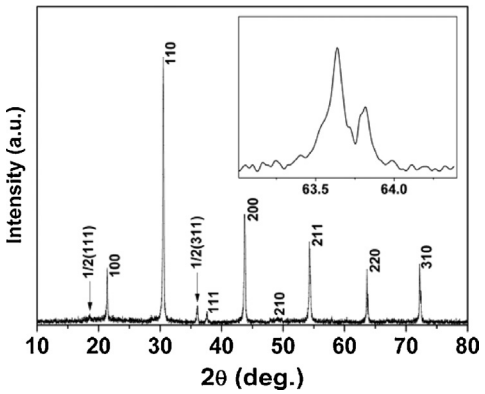

Fig. 2. X-ray powder diffraction patterns of the crashed PLN–0.2PT crystal with super-lattice reflections peak. The split in the fundamental lines around $2\theta = 64^\circ$ insert clearly show the orthorhombic phase.

with the purpose of high temperature application. The crystal with composition $x = 0.49$ shows high Curie temperature ($T_C = 360\,^\circ C$) and good piezoelectric properties ($d_{33} = 1630$ pC/N) [27]. The major studies of PLN–*x*PT crystal structures focus on the MPB region transition from Rhombohedral to Tetragonal phase. Broadening of the phase transition, dielectric dispersion, and the characteristic features of ferroelectric relaxors were observed within the concentration interval of $0.1 < x < 0.3$ in PLN–PT ceramics [24] and $x < 0.4$ in PLN–PT single crystals [27]. In these regions, PLN–PT system exhibits typical relaxor characteristics but the Curie temperature deviates from the ideal linear relationship between $0 < x < 1$. In this paper, the growth, structure and properties of PLN–0.2PT relaxor ferroelectric crystal are reported.

2. Experimental procedures

2.1. Crystal growth

Due to the high melting point of Lu_2O_3, a top seeded solid solution growth method was chosen to grow PLNT single crystal. Such a method also offers more advantages in growing single crystals of good quality and high compositional homogeneity. The flux is $PbO–H_3BO_3$. The starting chemicals and the ratios of flux to solute are described in Ref. [27]. The detailed growth process is similar to the one described by He et al. [28]. Finally, the single crystal has been obtained, as shown in Fig. 1.

2.2. Property characterization

The actual chemical compositions of the grown crystal was determined to be $x = 0.2$ by inductively coupled plasma atomic emission spectroscopy (*ICP-AES*, JY Ultima-2, France). The phase and structure of the grown crystal was carried out by X-ray diffraction analysis using Cu-Kα radiation (*DMAX*2500, Rigaku, Japan) at room temperature. Fine crystal powder for the electron microscopy study was polished mechanically and measured on a transmission electron microscope (TEM) (*Tecnai F20 FEG*, FEI, America). For electric characterization, the sample was sliced from the as-grown crystal along direction, polished and coated with silver paste as electrodes. Measurements of the dielectric constant and loss tangent (tanδ) were carried out by computer-controlled Alpha–broadband dielectric/impedance spectrometer (Novocontrol GmbH, Germany) with an AC signal of 0.5 V (peak-to-peak) applied. Polarization hysteresis loops were displayed by standard ferroelectric test system (TF Analyzer 2000E, *aix-ACCT*, Germany) at $f = 2$ Hz, combined with a high-voltage supply amplifier/controller (*Model 610E*, Trek, America) and an environmental test chamber (*DELTA 9023*, DELTA, America) with temperature varies from room temperature up to 130 °C. Poling was performed by applying a DC electric field of 20 kV/cm along the direction of the crystal at 60 °C for 15 min, and then keeping the field on while cooling down to room temperature. The piezoelectric coefficients were measured using a quasi-static

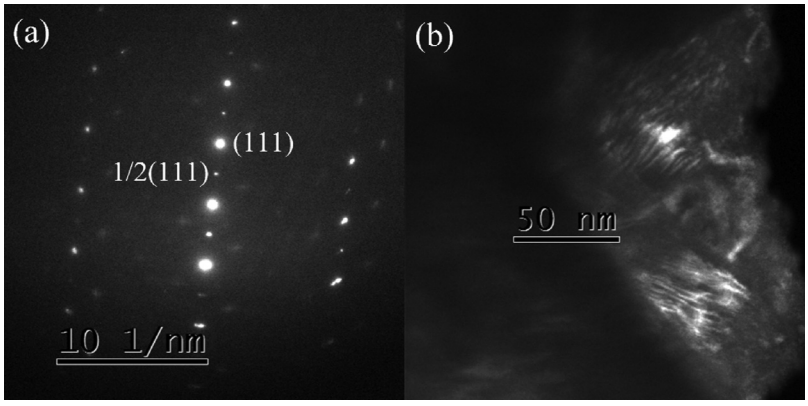

Fig. 3. Electron diffraction patterns of ferroelectric phase obtained (a) super-lattice reflections and (b) micro-domains configurations under TEM.

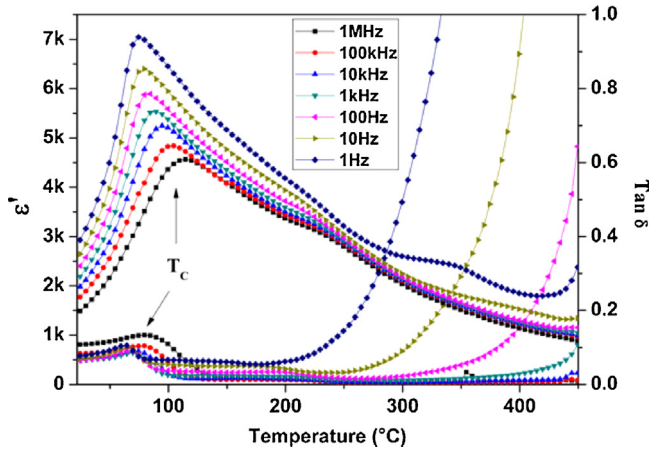

Fig. 4. The temperature dependence of the dielectric constant and loss tangent at various frequencies for unpoled <0 0 1>-oriented crystal.

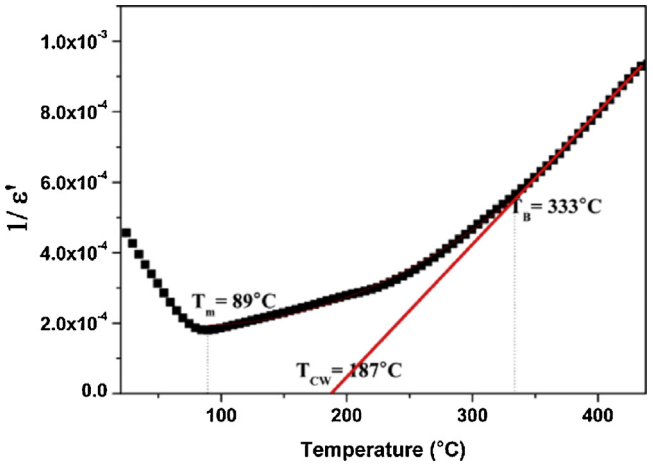

Fig. 5. Temperature dependence of $1/\varepsilon'$ at 1 kHz for PLN–0.2PT crystal fitted with the Curie–Weiss law.

d_{33} meter (Model: *ZJ-4AN* meter, Institute of Acoustics, Chinese Academy of Sciences).

3. Results and discussion

The photograph for the obtained PLN–0.2PT crystal is shown in Fig. 1, with (1 1 1) and (0 0 1) planes in habit, and a dark yellow color. The dimension of grown PLN–0.2PT crystal is larger than $10 \times 15 \times 11\ mm^3$ in size, generally. At room temperature, the X-ray diffraction pattern of PLN–0.2PT as shown in Fig. 2 exhibits typical perovskite structure. In addition, some super-lattice reflections also can be seen. The presence of super-lattice reflection suggests that the prototypic crystal structure is an ordered perovskite with an effective unit cell ($2a_c \times 2a_c \times 2a_c$) doubled in size in all crystallographic axis directions of a cubic, simple perovskite cell ($a_c \times a_c \times a_c$). Here, the subscript "c" refers to the cubic perovskite basis cell [23]. Pure PLN has a pronounced long-range order in the $A(B'_{1/2}B''_{1/2})O_3$-type '1:1' sublattice that arises from long range order of Lu^{3+} and Nb^{3+} cations. The compositions with 20 percent PT content exhibit super-lattice peaks, corresponding to d-spacing values twice as much as those of (1 1 1) and (3 1 1) major ones can be indexed as 1/2(1 1 1) and 1/2(3 1 1), respectively, showing short-range order feature of a single crystal. The short-range order may be determined by two factors: coexistence of chemically ordered and disordered regions, and incomplete ordering inside chemically ordered regions [29]. Special attention is focused on (2 2 0) peak. It is known that the XRD profiles of (2 2 0) reflections only shows a single peak R(2 2 0) in the rhombohedral structure because all the planes of (2 2 0) share the same lattice parameters. While in the orthorhombic phase, the (2 2 0) reflections would split into three peaks: the O(2 2 0), O(0 2 2) and O(2 0 2) profiles [30]. In the orthorhombic phase, the O(2 0 2) and O(0 2 2) peaks are so closed that the intensity of the O(2 0 2)/(0 2 2) peak is twice as that of the O(2 2 0) peak. As evidenced from the split in the fundamental lines around $2\theta = 64°$, shown in the insets of Fig. 2, the lattice distortion is found to be orthorhombic (space group Bmm2) in nature at room temperature. The previous work suggests that the phase structure of PLN–*x*PT at room temperature changes from orthorhombic (space group Bmm2) to rhombohedral (space group R3m) to tetragonal (space group P4mm) with the increasing *x*.

The super-lattice reflections are further identified by transmission electron microscopy as shown in Fig. 3(a). The pattern in Fig. 3(a) is composed of the fundamental spots of the prototype and the extra B-site atom ordering super-lattice reflection spots, corresponding to 1/2(1 1 1) and others. micro-domains configurations in PLN–0.2PT crystal is also studied using TEM. The electron beam heating often induces expansion of the wall and this changes the stability of the domains. Therefore, low accelerating voltages and low ion currents were used to prevent loss of PbO and in order not to modify domain configurations [31]. Finally

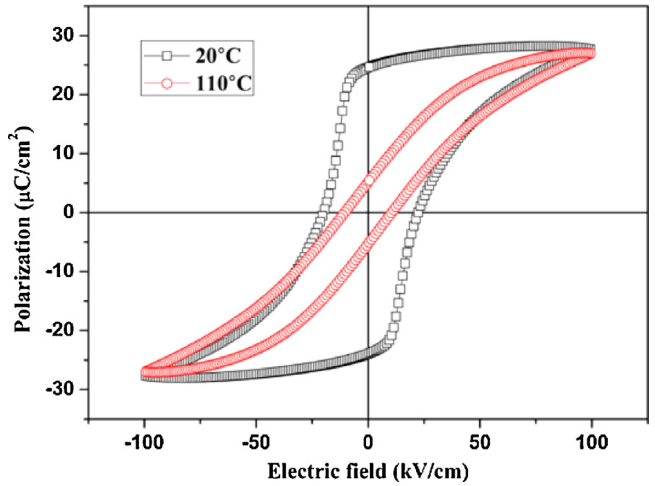

Fig. 6. Polarization vs. electric field loops for the $[1\,0\,0]_o$ plates PLN–0.2PT crystal at 20 °C and 110 °C (f = 2 Hz).

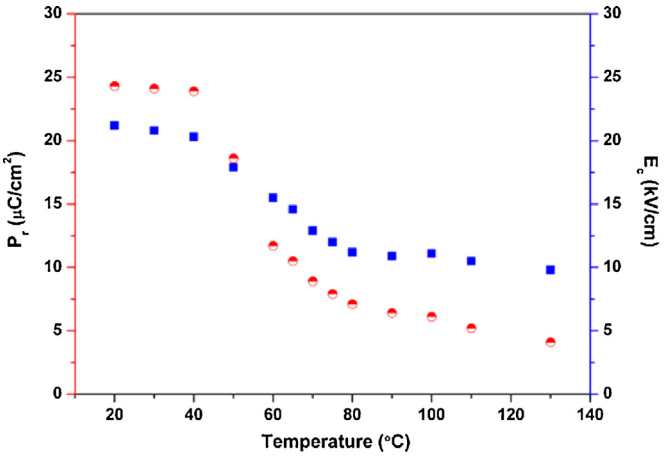

Fig. 7. Temperature dependence of E_C and P_r for the $[1\,0\,0]_o$ plates PLN–0.2PT crystal (f = 2 Hz).

ferroelectric micro-domains were clearly found with 1 ~ 2 nm in size, as shown in Fig. 3(b).

Fig. 4 shows the temperature dependence of the dielectric constant and loss tangent at various frequencies for unpoled <0 0 1>-oriented crystal plates. The room temperature values of the dielectric constant and loss tangent at 1 kHz are 2190 and 0.065, respectively. The dielectric constant of the crystal shows a broad maximum with frequency dispersion, the temperature of which shifts to higher temperature with increasing frequency, i.e. from 75 °C at 1 Hz to 115 °C at 1 MHz, indicating a typical relaxor behavior.

The dielectric behavior of ferroelectric materials is usually described by the Curie–Weiss law: $1/\varepsilon' = (T - T_{CW})/C$, where C is the Curie constant and T_{CW} is the Curie–Weiss temperature [32]. For normal ferroelectrics at temperature above T_C, the dielectric constant $1/\varepsilon'$ obeys the Curie–Weiss law. However, the temperature dependence of dielectric constant ε' above T_C deviates from the Curie–Weiss law due to short-range correlations between PNRs, which are inherent in the relaxor ferroelectrics [4,33,34]. Fig. 5 shows the temperature dependence of $1/\varepsilon'$ at 1 kHz for the as grown crystal. It can be seen that the real permittivity obeys the Curie–Weiss law only above the Burns temperature T_B, below which the dielectric behavior deviates from the Curie–Weiss law. The value of T_{CW} is higher than its T_C. The values of T_{CW} and T_B are 187 °C and 333 °C, respectively. It is known that the PNRs start to form when the temperature is below T_B [35]. This dielectric behavior indicates that the PLN–0.2PT crystal is of relaxor-type and the ferroelectric–paraelectric transition at T_C is a diffuse phase transition, which is consistent with that of relaxors [33,36].

The polarization-electric field (P–E) hysteresis loops of PLN–0.2PT crystal platelet along <0 0 1>-oriented at 20 °C and 110 °C are displayed in Fig. 6. It is found that the PLN–0.2PT crystal exhibits saturated loops at temperature below and above Curie temperature T_C (75 °C at 1 Hz and 80 °C at 10 Hz based on the dielectric spectra of Fig. 4, respecitively) at $f = 2$ Hz, indicating typical relaxor ferroelectric behavior. The temperature dependences of the remnant polarizations P_r with a coercive electric field of E_C under a bipolar drive of $E = \pm 100$ kV/cm at 2 Hz was shown in Fig. 7. The values of E_C and P_r decrease with the increase of temperature. The piezoelectric coefficient d_{33} is obtained to be 115pC/N at room temperature.

4. Conclusions

Single crystal of $Pb(Lu_{1/2}Nb_{1/2})O_3$–$0.2PbTiO_3$ is successfully grown by TSSG method using PbO–H_3BO_3 flux. The crystal structure is found to be orthorhombic in nature as revealed by the analysis of the XRD date at room temperature. In addition, some super-lattice reflections are found due to short range ordering of B-site cations. The super-lattice reflections are further identified by TEM. Micro-domains configurations in PLN–0.2PT crystal is also studied using TEM with 1~2 nm in size. The temperature dependence of the dielectric constant (ε') and the temperature dependence of $1/\varepsilon'$ further confirm the typical relaxor behavior. The values of E_C and P_r decrease with the increase of temperature but still exists above the T_C. This suggests that, the PLN–0.2PT single crystal is a typical relaxor ferroelectric crystal. Further investigation would be done on obtaining larger single crystals with more components near or within the region $x < 0.2$ in order to obtain a more accurate phase diagram and to study the transition from anti-ferroelectric phase to ferroelectric phase.

Acknowledgments

This work is supported by the National Natural Science Foundation of China under Grant no. 11404331 and the Youth Innovation Funding of Fujian Province (2014J05069).

References

[1] L.E. Cross, Ferroelectrics 76 (1987) 241.
[2] L.E. Cross, Ferroelectrics 151 (1994) 305.
[3] A.A. Bokov, Z.-G. Ye, Phys. Rev. B 74 (2006) 132102.
[4] A.A. Bokov, Z.-G. Ye, J. Mater. Sci. 41 (2006) 31.
[5] C.A. Randall, A.S. Bhalla, T.R. Shrout, L.E. Cross, J. Mater. Res. 5 (1990) 829.
[6] B.E. Vugmeister, H. Rabitz, Phys. Rev. B 57 (1998) 7581.
[7] G.A. Smolenskii, V.A. Isupov, A.I. Agranovskaya, S.N. Popov, Sov. Phys. Solid State 2 (1961) 2584.
[8] F. Chu, N. Setter, A.K. Tagantsev, J. Appl. Phys. 74 (1993) 5129.
[9] X.F. Long, Z.G. Ye, Acta Mater. 55 (2007) 6507.
[10] M. Dong, Z.G. Ye, J. Cryst. Growth 209 (2000) 81.
[11] S.E. Park, T.R. Shrout, J. Appl. Phys. 82 (1997) 1804.
[12] L.C. Lim, K.K. Rajan, J. Cryst. Growth 271 (2004) 435.
[13] I. Makoto, A. Takashi, M. Masaki, S. Ikuo, O. Hidehiro, Y. Naohiko, O. Hiroshi, I. Yoshihiro, Jpn. J. Appl. Phys. 41 (2002) 7003.
[14] S. Saitoh, T. Kobayashi, K. Harada, S. Shimanuki, Y. Yamashita, IEEE Trans. Ultrason. Ferroelectr. Freq. Control 45 (1998) 1071.
[15] Y. Naohiko, O. Hidehiro, K. Motoyuki, H. Yasuharu, Y. Yohachi, I. Shinnichirou, T. Hikaru, I. Makoto, I. Yoshihiro, Jpn. J. Appl. Phys. 40 (2001) 5664.
[16] S.J. Zhang, P.W. Rehrig, C. Randall, T.R. Shrout, J. Cryst. Growth 234 (2002) 415.
[17] Y. Yamashita, S. Shimanuki, Mater. Res. Bull. 31 (1996) 887.
[18] Y.H. Bing, Z.G. Ye, J. Cryst. Growth 250 (2003) 118.
[19] Y.H. Bing, Z.G. Ye, J. Cryst. Growth 287 (2006) 326.
[20] N. Yasuda, H. Ohwa, D. Hasegawa, K. Hayashi, Y. Hosono, Y. Yamashita, M. Iwata, Y. Ishibashi, Jpn. J. Appl. Phys. 39 (2000) 5586.
[21] Y.P. Guo, H.S. Luo, T.H.Z. He, W. Yin, Solid State Commun. 123 (2002) 417.
[22] D.Q. Shen, X.Z. Li, Z.J. Wang, Y. Liu, C. He, T. Li, X.F. Long, J. Eur. Ceram. Soc. 32 (2012) 1077.
[23] Y. Park, J. Am. Ceram. Soc. 83 (2000) 135.
[24] M. Antonova, L. Shebanovs, M. Livinsh, J.Y. Yamashita, A. Sternberg, I. Shorubalko, A. Spule, J. Electroceram. 4 (2000) 179.
[25] A. Sternberg, L. Shebanovs, M. Antonova, M. Livinsh, J.Y. Yamashita, L. Shombalko, A. Spule, Nanostruct. Mater. 12 (1999) 645.
[26] A. Sternberg, L. Shebanovs, E. Birks, Y. Yamashita, M. Tyunina, V. Zauls, Ferroelectrics 217 (1998) 307.
[27] Y. Liu, X.Z. Li, Z.J. Wang, C. He, T. Li, L.D. Ai, T. Chu, D.F. Pang, F. Long, CrystEngComm 15 (2013) 1643.
[28] C. He, X.Z. Li, Z.J. Wang, X.F. Long, S.Y. Mao, Z.G. Ye, Chem. Mater. 22 (2010) 5588.
[29] X.F. Long, A.A. Bokov, Z.G. Ye, W. Qu, X. Tan, J. Phys. Condens. Matter 20 (2008) 015210.
[30] Z.G. Xia, Q. Li, Solid State Commun. 142 (2007) 323.
[31] H. Fuiishita, Y. Shiozaki, N. Achiwa, E. Sawaeuchi, Phys. Soc. Jpn. 51 (1982) 3583.
[32] P.B. Pokharel, D. Pandey, J. Appl. Phys. 88 (2000) 5364.
[33] D. Viehland, S.J. Jang, L.E. Cross, M. Wuttig, Phys. Rev. B: Condens. Matter 46 (1992) 8003.
[34] A.A. Bokov, Z.-G. Ye, Phys. Rev. B: Condens. Matter 66 (2002) 064103.
[35] C. He, X.Z. Li, Z.J. Wang, Y. Liu, D.Q. Shen, T. Li, X.F. Long, CrystEngComm 14 (2012) 4513.
[36] A.A. Bokov, Z.G. Ye, Appl. Phys. Lett. 77 (2000) 1888.